



Contents lists available at ScienceDirect

International Journal of Solids and Structures

journal homepage: www.elsevier.com/locate/ijsolstr

A smoothed inverse eigenstrain method for reconstruction of the regularized residual fields

S. Ali Faghidian*

Department of Mechanical and Aerospace Engineering, Science and Research Branch, Islamic Azad University, Tehran, Iran

ARTICLE INFO

Article history:

Received 22 July 2014

Received in revised form 15 September

2014

Available online xxxx

Keywords:

Residual stress

Inverse problems

Eigenstrain

Tikhonov–Morozov regularization

Gradient iterative regularization

ABSTRACT

A smoothed inverse eigenstrain method is developed for reconstruction of residual field from limited strain measurements. A framework for appropriate choice of shape functions based on the prior knowledge of expected residual distribution is presented which results in stabilized numerical behavior. The analytical method is successfully applied to three case studies where residual stresses are introduced by inelastic beam bending, laser-forming and shot peening. The well-rehearsed advantage of the proposed eigenstrain-based formulation is that it not only minimizes the deviation of measurements from its approximations but also will result in an inverse solution satisfying a full range of continuum mechanics requirements. The smoothed inverse eigenstrain approach allows suppressing fluctuations that are contrary to the physics of the problem. Furthermore, a comprehensive discussion is performed on regularity of the asymptotic solution in the Tikhonov scheme and the regularization parameter is then exactly determined utilizing Morozov discrepancy principle. Gradient iterative regularization method is also examined and shown to have an excellent convergence to the Tikhonov–Morozov regularization results.

© 2014 Elsevier Ltd. All rights reserved.

1. Introduction

Residual stresses are generated in engineering structures as a result of a variety of manufacturing processes. So it is important to correctly quantify Residual stress field to determine the integrity and durability of an engineering structure. It is also well known that uncontrolled residual stresses are detrimental to the performance and lifetime of engineering components (Withers, 2007). The residual stresses in engineering structures are generally determined by interpretation of experimental measurements or process modeling where major limitations exist in both approaches (Jun and Korsunsky, 2010). Residual stresses can be measured using various experimental methods (Withers et al., 2008) introducing uncertainty on the residual field distribution. Although statistical methods (Faghidian, 2013; Wimpory et al., 2009) provide confidence intervals on the measured residual stress distribution but the results do not satisfy the necessary continuum mechanics requirements. Theory of inverse methods has been developed over the past decades and gained a great attention including determination of residual stress field from limited experimental measurements (Ma et al., 2012). The inverse eigenstrain method is a semi-empirical approach based on the theory of eigenstrains that

combines experimental characterization in terms of residual elastic strains. The general framework of inverse problem of eigenstrain approach was introduced by Hill (1996), Cao et al. (2002) and Qian et al. (2004). The approach was then developed by Korsunsky (2005, 2006), Korsunsky et al. (2007) investigating various aspects of the framework and a least squares approach was used to determine unknown eigenstrain distributions from limited measurements of residual elastic strains. A detail description of the inverse eigenstrain approach is given by Jun and Korsunsky (2010). An alternative approach, which does not utilize assumed eigenstrain distribution, is to introduce a series of stress functions that directly solve the stress equilibrium equations together with traction free boundary conditions. In a series of publications (Farrahi et al., 2009a,b, 2010; Faghidian et al., 2012a,b) the stress function approach that does not require numerical tools such as the finite element or boundary element methods, successfully reconstruct the complete residual stress field in a variety of processes and geometries. Recently Coules et al. (2014) introduced a finite element based method for reconstruction of general three-dimensional residual stress distribution from measurements made in an incompatible region without determination of the eigenstrain distribution. Also Nedin and Vatulyan (2013) proposed analytical solution for the vibration of thin plates with non-homogeneous pre-stress fields to reconstruct residual stresses by the acoustical method.

* Tel./fax: +98 21 44868536.

E-mail address: Faghidian@gmail.com

It is well known that the residual stresses may not be measured directly and experimental methods typically measure the distortion and hence strain in the specimen (Faghidian et al., 2012a,b). In the present study, variational inverse eigenstrain approach would be reconsidered and modified to reconstruct the residual elastic strain, stress and eigenstrain field from experimental strain measurements. The proposed smoothed inverse eigenstrain approach results in non-singular and smooth reconstructed residual fields while satisfying all of the continuum mechanics requirements. A framework for appropriate choice of non-linear shape functions based on the prior knowledge of the expected distribution is also presented in three different process of inelastic beam bending, laser-forming and shot peening. Furthermore, a comprehensive discussion is performed on the various mathematical aspect of the numerical reconstruction consisting of invertibility, uniqueness, well-posedness and convergence of the asymptotic residual field solution. The regularity of the approximated solution is also completely discussed in the Tikhonov scheme and the regularization parameter is then exactly determined utilizing Morozov discrepancy principle. Moreover since iterative regularization methods are known to be an attractive alternative to Tikhonov regularization, gradient iterative method is examined here and the results are compared to Tikhonov–Morozov regularization for the level of accuracy and the rate of convergence issues.

2. Smoothed inverse eigenstrain analysis

2.1. Residual stresses

Residual stresses are generally characterized as the stress field supported in a continuum with a fixed reference configuration where there is no external forces and thermal gradients (Hoger, 1986). The region of interest containing the distribution of longitudinal residual stress $\sigma_{xx} = \sigma(z)$ is a plate infinitely extended in x direction with depth of h in the z direction. The plate geometry is illustrated in Fig. 1. All residual stresses and strains are assumed to be independent of x and y and only dependent on z coordinate. This is similar to the approach adopted in earlier works (Korsunsky, 2005, 2006) to examine residual stress field in beams and plates.

The residual stress field must satisfy the equilibrium equations in the absence of body forces which is described as $\sigma_{ij,j} = 0$ in plane Cartesian coordinates. Furthermore the traction free boundary conditions should also be satisfied as $\sigma_{ji}n_j = 0$ where \mathbf{n} denotes the outward unit surface normal (Timoshenko and Goodier, 1970). A necessary condition for residual stresses is that the Cartesian components of the mean residual stress are always zero, so $\int_V \sigma_{ij}dV = 0$ where V is the volume of the continuum (Mura, 1987). The zero mean residual stress for the introduced domain reduces to,

$$\int_0^h \sigma_{xx}(z)dz = 0 \tag{1}$$

Following the stress function approach (Faghidian et al., 2012a,b), an appropriate form of the Airy stress function is given by a truncated series that satisfies the stress equilibrium equations



Fig. 1. Illustration of the problem geometry.

together with the traction free boundary conditions and the mean residual stress over the entire domain is zero. The proposed Airy stress function for the domain of interest is given by,

$$\varphi(z) = z^2(z-h)^2 \left[\sum_{m=1}^M c_m f_m(z) \right] \tag{2}$$

where c_m are unknown real coefficients yet to be determined and $f_m(z)$ is a series of shape functions to be selected based on the prior knowledge of the expected distribution of residual stress field. Also note that the shape functions of $f_m(z)$ should have at least continuous derivatives over the entire domain. Therefore, utilizing the Airy stress function would result in the final form of the longitudinal residual stress as,

$$\begin{aligned} \sigma_{xx}(z) &= \frac{\partial^2 \varphi(z)}{\partial z^2} = \sum_{m=1}^M c_m \psi_m(z) \\ &= 2(h^2 - 6hz + 6z^2) \left[\sum_{m=1}^M c_m f_m(z) \right] \\ &\quad + 4z(h^2 - 3hz + 2z^2) \left[\sum_{m=1}^M c_m f'_m(z) \right] \\ &\quad + z^2(z-h)^2 \left[\sum_{m=1}^M c_m f''_m(z) \right] \end{aligned} \tag{3}$$

Since the domain of interest coincides on the x - z plane, no gradient in the y direction is allowed. Hence for both conditions of the plane-stress and plane-strain, the reconstructed in-plane residual stress state is credible. Also it should be noted that the smoothed inverse eigenstrain method works independent of the constitutive material behavior and the plate bending theory assumptions. The kinematics of the deformation in terms of the strain compatibility equations would be completely discussed in Section 2.2. Nonetheless, the static equilibrium across the continuum domain expressed in terms of resultant force and moment is also guaranteed respectively as,

$$\begin{aligned} \int_0^h \sigma_{xx}(z)dz &= \int_0^h \frac{\partial^2 \varphi(z)}{\partial z^2} dz = \frac{\partial \varphi(z)}{\partial z} \Big|_0^h = 0 \\ \int_0^h z \sigma_{xx}(z)dz &= \int_0^h z \frac{\partial^2 \varphi(z)}{\partial z^2} dz = z \frac{\partial \varphi(z)}{\partial z} \Big|_0^h - \frac{\partial \varphi(z)}{\partial z} \Big|_0^h = 0 \end{aligned} \tag{4}$$

It will be shown in the Section 2.2 that the stress function approach, developed by the author (Faghidian et al., 2012a,b), could be appropriately modified to reconstruct the residual elastic strain and eigenstrain field from limited strain measurements.

2.2. Residual elastic strains

The direct problem of eigenstrain is known as the problem of determination of residual stresses resulting from a known eigenstrain distribution utilizing generalized Hooke's law (Korsunsky, 2009). The residual stress field is well known to depend on the internal incompatibility within the continuum. The distribution of incompatible strain field in such a continuum is known as the eigenstrain distribution, and it is generally assumed that total strain tensor ϵ_{ij} can be expressed as the sum of the elastic e_{ij} and eigenstrain terms ϵ_{ij}^* as (Mura, 1987),

$$\epsilon_{ij} = e_{ij} + \epsilon_{ij}^* \tag{5}$$

According to Korsunsky (2006), in the absence of external loading being applied, elastic strain presents an illustration of residual elastic strain (R.E.S.), such as that measured in a diffraction experiments. Also Kinematic analysis of continuous deformation requires the strain field to be compatible. Hence, the total strain

compatibility equation in general form, $\varepsilon_{ik,jl} + \varepsilon_{jl,ik} - \varepsilon_{jk,il} - \varepsilon_{il,jk} = 0$, for the introduced domain is reduced to (Timoshenko and Goodier, 1970),

$$\frac{d^2 \varepsilon_{xx}(z)}{dz^2} = 0 \quad (6)$$

Thus to satisfy the strain compatibility equation in general form, total strain should be a linear function of z . The key concept of inverse eigenstrain approach is that, the residual stress components are proportional to the R.E.S. (Korsunsky, 2006). Therefore utilizing generalized Hooke's law, the longitudinal component of the residual stress may be shown to be

$$\sigma_{xx}(z) = \tilde{E} \varepsilon_{xx}(z) \quad (7)$$

where $\tilde{E} = E$ for plane-stress, $\tilde{E} = E/(1 - \nu^2)$ for plane-strain and $\tilde{E} = E/(1 - \nu)$ for biaxial-stress state (Korsunsky, 2005) with E and ν are the Young's modulus and Poisson's ratio of the material, respectively. Finally the proportionality assumption will result in a truncated series form of the longitudinal R.E.S. having the same shape functions as the residual stresses,

$$\begin{aligned} \varepsilon_{xx}(z) = & \sum_{m=1}^M \lambda_m \psi_m(z) = 2(h^2 - 6hz + 6z^2) \left[\sum_{m=1}^M \lambda_m f_m(z) \right] \\ & + 4z(h^2 - 3hz + 2z^2) \left[\sum_{m=1}^M \lambda_m f'_m(z) \right] \\ & + z^2(z - h)^2 \left[\sum_{m=1}^M \lambda_m f''_m(z) \right] \end{aligned} \quad (8)$$

The truncated series form of the longitudinal R.E.S. distribution clearly satisfies the static equilibrium across the domain due to its proportionality to residual stresses.

2.3. Eigenstrains

Since there are no continuum requirements on the form of the eigenstrain distribution, the series form of the longitudinal eigenstrain $\varepsilon_{xx}^*(z)$ could be expressed in terms of the smooth and appropriately localized eigenstrain base functions $\psi_m^*(z)$, as

$$\varepsilon_{xx}^*(z) = \sum_{m=1}^M \lambda_m \psi_m^*(z) \quad (9)$$

However the longitudinal component of the total strain should have the linear form of $\varepsilon_{xx}(z) = k_0 + k_1 z$ to satisfy the strain compatibility equation. Therefore if the measurement data are available in the eigenstrain form then the R.E.S. distribution would be expressed as,

$$\varepsilon_{xx}(z) = \varepsilon_{xx}(z) - \varepsilon_{xx}^*(z) = (k_0 + k_1 z) - \sum_{m=1}^M \lambda_m \psi_m^*(z) \quad (10)$$

It is well known that the choice of eigenstrain base functions is arbitrary while the R.E.S. field must satisfy the continuum mechanics requirements expressed here in terms of the static equilibrium across the domain. So the unknown coefficients of k_0 and k_1 would be determined by satisfying the force and moment balance across the domain (Korsunsky, 2006) as,

$$\begin{aligned} k_0 &= \frac{2}{h^2} \int_0^h \varepsilon_{xx}^*(z)(2h - 3z) dz \\ k_1 &= -\frac{6}{h^3} \int_0^h \varepsilon_{xx}^*(z)(h - 2z) dz \end{aligned} \quad (11)$$

It is also important to note that the proposed series form of the R.E.S. and eigenstrains not only will result in satisfying the continuum requirements but also produce a smoothed nonsingular

residual stress field having the ability of imposing more physical conditions. Furthermore it should be emphasized that the linear form of the total strain is due to satisfy the strain compatibility equations and is valid independent of the plate bending theory assumptions.

2.4. Least squares approximation

If the eigenstrain distribution and elastic properties of a continuum are known, the residual stress field can be determined directly. Solution of the direct eigenstrain problem has widespread application in engineering and micromechanics (Mura, 1987). To achieve the best values for the coefficients of λ_m appearing in the asymptotic expansion of residual elastic strain, R.E.S., a least squares approximation analysis is developed here. Provided a limited set of experimental data consisting of the values of R.E.S. as E_n are measured at positions z_n , then evaluating the shape function of $\psi_m(z)$ at each n measurement positions of z_n , results in predicted values of $\psi_{mn} = \psi_m(z_n)$. The following functional error that is the sum of squares of deviations of the observed values of E_n from its predicted values Ψ_{mn} , should be minimized,

$$J = (\Psi^T \Lambda - \mathbf{E})^T (\Psi^T \Lambda - \mathbf{E}) \quad (12)$$

where the matrix notation of $\Psi = [\psi_{mn}]$, $\Lambda = \{\lambda_m\}$ and $\mathbf{E} = \{E_n\}$ are introduced over the $n = 1 \dots N$ measurement points and $m = 1 \dots M$ the number of truncated series used to approximate the residual elastic strain field and the superscript T refers to the transposed form of a matrix. Also the gradient of the functional error with respect to coefficients Λ may be shown to be,

$$\nabla_j J = 2\Psi(\Psi^T \Lambda - \mathbf{E}) \quad (13)$$

Hence, unique values of coefficients Λ can be determined by setting the gradient of the functional with respect to coefficients equal to zero,

$$\Lambda = [\Psi\Psi^T]^{-1} \Psi\mathbf{E} \quad (14)$$

Although the residual stress field in a continuum is not uniquely defined by the geometry, material behavior and boundary conditions as is the case for stress field arising solely from external loading (Timoshenko and Goodier, 1970). Instead in approximation theory, it can be shown that in an inner product space, if a set of shape functions is linearly independent then the symmetric positive-definite matrix $\Psi\Psi^T$ is nonsingular and the uniqueness of the solution in the sense of a least squares approximation is guaranteed (Cheney, 1982). To check linear independency of the set of shape functions $\psi_m(z)$, the Wronskian determinant of this set is tested numerically on the interval $[0, h]$ and there is at least one point where the Wronskian is not equal to zero. Hence this set must be linearly independent.

To quantify the accuracy of the numerical computations, a practical footnote is also addressed here. The well-posedness of the solution utilizing the present method is related to the condition number of the system of linear equations appearing in the equation of $\nabla_j J = 0$. If the condition number of matrix $\Psi\Psi^T$ is small, where "small" means roughly the condition number to have the less order of the of matrix entries, then the numerical linear system is well-posed and has a well numerical behavior (Allaire and Kaber, 2008).

Also for each continuous function there corresponds a formal expansion which has the property that its partial sums is the best approximations to the function in the least squares sense. It can be shown that this partial sum in the least squares sense will always converge to the function under the conditions of linear independency of the shape functions (Cheney, 1982) that is already

satisfied here. However the rate of convergence for the asymptotic solution would be studied numerically in Section 3.

At last it should be noted that when the measurement data are available in the eigenstrain form \mathbf{E}^* instead of R.E.S. measurements \mathbf{E} , similar least square analysis would be utilized to determine the coefficients of Λ while the R.E.S. shape functions would be replaced by the eigenstrain base functions and the coefficients would be evaluated as $\Lambda = [\Psi^*(\Psi^*)^T]^{-1} \Psi^* \mathbf{E}^*$.

2.5. Regularization

In regularity discussion of the approximate solution, the focus is on the issue of continuous dependence on the measured data. Among many different regularization methods, perhaps the classic and most familiar is Tikhonov method. Tikhonov regularization method takes the output least squares formulation, Eq. (12), and adds a stabilizing term to the least squares functional (Tikhonov and Arsenin, 1977). Finally the Tikhonov functional $J(\alpha)$ is defined as,

$$J(\alpha) = (\Psi^T \Lambda(\alpha) - \mathbf{E})^T (\Psi^T \Lambda(\alpha) - \mathbf{E}) + \alpha \Lambda^T(\alpha) \Lambda(\alpha) \quad (15)$$

where the positive parameter of α is known as the Tikhonov regularization parameter. Unique values of coefficients $\Lambda(\alpha)$ can be found by minimizing the Tikhonov functional,

$$\nabla_{\Lambda(\alpha)} J = 2\Psi(\Psi^T \Lambda(\alpha) - \mathbf{E}) + 2\alpha \Lambda(\alpha) = 0 \quad (16)$$

Therefore the regularized coefficients may be shown to be,

$$\Lambda(\alpha) = [\Psi \Psi^T + \alpha \mathbf{I}]^{-1} \Psi \mathbf{E} \quad (17)$$

where \mathbf{I} is the identity matrix. Although in the class of bounded solutions, it may be shown that the approximate solution in the Tikhonov scheme converges to the exact solution but the Tikhonov regularization method does not allow one to explicitly give the optimal value of regularization parameter (Samaraskii and Vabishchevich, 2007). However the appropriate choice of the regularization parameter is primarily important, since its value needs to be properly matched with measured data inaccuracies. In fact, a regularization method should give an alternate method of constructing an approximate solution for which it is guaranteed the convergence of the regularized solution to exact solution as the noise level δ converges to zero. Among different criteria for choosing the regularization parameter, perhaps Morozov discrepancy principle (Morozov, 1984) is the most popular. The regularization parameter is chosen so that the norm of the discrepancy is of the order of the noise in data. The heuristic motivation of the principle is that the method should not produce results more accurate than the level of error in the given data, so according to the Morozov discrepancy principle,

$$\delta^2 = \frac{1}{N} (\Psi^T \Lambda(\alpha) - \mathbf{E})^T (\Psi^T \Lambda(\alpha) - \mathbf{E}) \quad (18)$$

In practice, the measurement error δ is not generally reliably known and values previously determined by the measurement equipment manufacturer or experimenters may not be utilized. However, a good estimate for the measurement error in Morozov discrepancy principle could be the unbiased estimator for variance of the measured data (Faghidian et al., 2014). Hence the governing equation on the Tikhonov regularization parameter according to Morozov discrepancy principle is,

$$(\Psi^T \Lambda(\alpha) - \mathbf{E})^T (\Psi^T \Lambda(\alpha) - \mathbf{E}) = \frac{N}{N-2} (\Psi^T [\Psi \Psi^T]^{-1} \Psi \mathbf{E} - \mathbf{E})^T (\Psi^T [\Psi \Psi^T]^{-1} \Psi \mathbf{E} - \mathbf{E}) \quad (19)$$

where the regularized coefficients of $\Lambda(\alpha)$ had been already evaluated as Eq. (17).

Iterative regularization methods are recently investigated extensively and it seems that they are an attractive alternative to Tikhonov regularization technique. The major advantage of iteration methods over the Tikhonov regularization is that they need no special definition of the regularization parameter. Among different iterative methods, the methods based on the minimization of the functional error J by gradient descent methods is one of the most effective and commonly used (Bakushinsky et al., 2011). In gradient descent method, by varying the descent step size γ_m and adjusting the direction of the descent, minimizing sequence could be constructed as (Kabanikhin, 2012),

$$\Lambda_{m+1} = \Lambda_m - \gamma_m \nabla_{\Lambda} J(\Lambda_m) \quad (20)$$

where the descent parameter of γ_m could be determined by minimizing the function of $J(\Lambda_{m+1})$ as (Kabanikhin, 2012),

$$\gamma_m = \frac{(\nabla_{\Lambda} J(\Lambda_m))^T (\nabla_{\Lambda} J(\Lambda_m))}{2(\Psi^T \nabla_{\Lambda} J(\Lambda_m))^T (\Psi^T \nabla_{\Lambda} J(\Lambda_m))} \quad (21)$$

It is also important to estimate the rate of convergence and to have a stopping criterion for the iterative process. The most commonly used criterion is Morozov discrepancy principle which is based on the credible speculation that it is probably not worth continuing the process after the residual $(1/N)(\Psi^T \Lambda_m - \mathbf{E})^T (\Psi^T \Lambda_m - \mathbf{E})$ becomes less than the measurement error δ . In other word, Morozov discrepancy principle determines that the iterative method does not have mathematical meaning to be continued after the residual of approximation and measured data becomes less than the measurement error (Bakushinsky et al., 2011; Kabanikhin, 2012). It should be noted that the initial guess for coefficients Λ_0 is usually chosen on the basis of some a priori information about the solution and here the initial guess of coefficients is chosen to be un-regularized coefficient of Eq. (14) as $\Lambda_0 = [\Psi \Psi^T]^{-1} \Psi \mathbf{E}$.

Finally it should be noted that the regularized coefficients of $\Lambda(\alpha)$ could be determined by the similar regularization analysis for the reconstruction of the eigenstrain field, replacing the R.E.S. shape functions with the eigenstrain base functions and the regularized coefficients would be evaluated as $\Lambda(\alpha) = [\Psi^*(\Psi^*)^T + \alpha \mathbf{I}]^{-1} \Psi^* \mathbf{E}^*$.

3. Reconstruction results and discussion

The new framework of smoothed inverse eigenstrain method developed in the previous sections would be applied to three experimental data sets here. First the residual elastic strain measurements in an inelastic bent beam using high energy synchrotron X-ray diffraction studied by Korsunsky (2006) would be examined. The Ti-6Al-4V alloy specimen had the length of 50 mm, thickness of 8.5 mm and depth of 4 mm and bent under four point bending conditions. The X-ray diffraction strain measurements and the reconstruction results of high order approximation of residual elastic strain by the variational inverse eigenstrain method (Korsunsky, 2006) are shown in Fig. 2. However to reconstruct the residual elastic strain utilizing smoothed inverse eigenstrain method, the mathematical form of the shape functions of $f_m(z)$ must be first determined base on the physical conditions of the inelastic bending residual stress field. The residual stress field through the thickness of inelastic bent steel beam is also studied by Faghidian et al. (2012a) utilizing the stress function approach and the Chebyshev polynomial of the second kind is shown to be an excellent choice for shape functions. So for the measurements shown in Fig. 2, similar to the stress function approach, the shape functions are selected to be $f_m(z) = T_{m-1}(z)$ where Chebyshev polynomial of the second kind are defined as $T_m(z) = \cos(m \cos^{-1}(z))$. The coefficients of Λ are then determined and consequently the residual

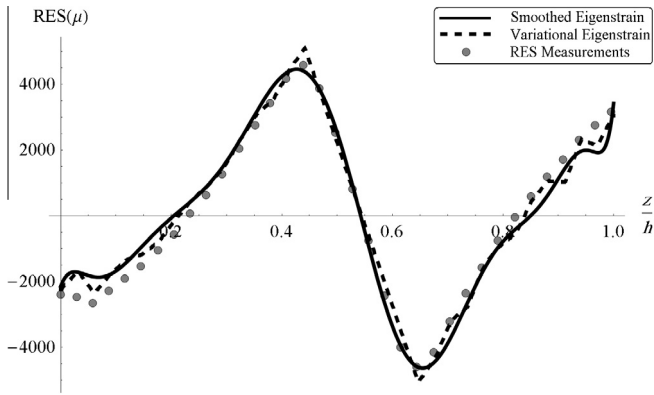


Fig. 2. R.E.S. measurements (Korsunsky, 2006) compared with the reconstructed RES by variational (Korsunsky, 2006) and smoothed inverse eigenstrain analysis.

elastic strain distribution given by Eq. (8) is reconstructed and exhibited in Fig. 2.

The order of polynomials used for reconstruction of residual elastic strain by variational inverse eigenstrain analysis is $M = 10$ (Korsunsky, 2006) while the order of the Chebyshev polynomial utilized for shape functions in smoothed inverse eigenstrain method is $M = 12$. It is clearly deduced from Fig. 2 that both reconstructions have an excellent agreement with the experimental measurements. However it should be noted that the reconstructed R.E.S. profile by smoothed inverse eigenstrain method has the higher order polynomials with less fluctuating numerical behavior. Also due to the asymmetry of titanium plastic behavior in tension and compression, residual elastic strain state is asymmetric (Korsunsky, 2006). Therefore in contrast to anti-symmetric residual stress field of steel bent beam (Faghidian et al., 2012a) both even and odd terms of Chebyshev polynomial are utilized here. Also to regularize the reconstructed residual strain field using Tikhonov method, first the regularization parameter should be determined using Eq. (19), afterward the regularized coefficients $\Lambda(\alpha)$ would be determined according to Eq. (17). The regularized R.E.S. fields by Tikhonov–Morozov regularization method together with the results of the gradient iterative regularization method are shown in Fig. 3. It is obviously inferred from Fig. 3 that the gradient iterative method has an excellent convergence to the Tikhonov–Morozov regularization results and the level of accuracy of the iterative regularization may be expressed as follows,

$$\frac{(\Lambda_{reg} - \Lambda_{itr})^T (\Lambda_{reg} - \Lambda_{itr})}{\Lambda_{reg}^T \Lambda_{reg}} \quad (22)$$

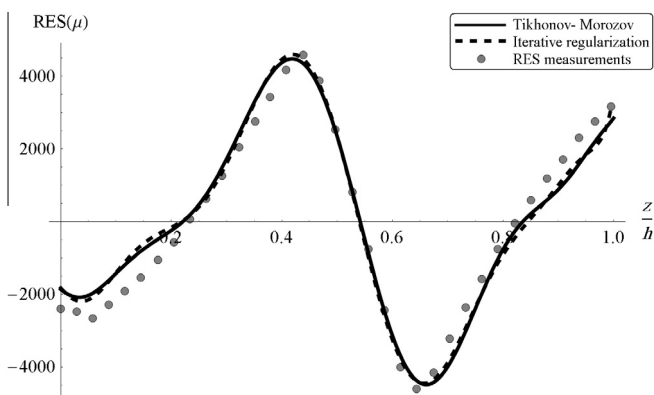


Fig. 3. R.E.S. measurements (Korsunsky, 2006) compared with the regularized reconstructed R.E.S. by Tikhonov–Morozov and iterative regularization method.

where Λ_{reg} and Λ_{itr} are the regularized coefficients according to Tikhonov–Morozov and gradient iterative regularization method, respectively. The regularization parameter, iteration steps and regularization relative error are given in Table 1.

The second residual elastic strain field considered here are the R.E.S. measurements in laser-formed steel plate using synchrotron X-ray diffraction studied by Korsunsky et al. (2008). The mild steel SABS 1431 plate was under hot rolling followed by laser bending process. A rectangular test samples with dimensions of $200 \times 60 \times 8$ mm were cut from the plates and treated with three laser passes along the center-line of one face perpendicular to the long side. The X-ray diffraction strain measurements and the R.E.S. approximation achieved using line-wise bending approximation through the thickness coordinate by the variational inverse eigenstrain analysis (Korsunsky et al., 2008) are shown in Fig. 4. However in the framework of smoothed inverse eigenstrain method, the physical conditions of the laser-forming residual stresses must be applied to the shape functions. Similar to the stress function approach (Farrahi et al., 2009a,b), first a modulation function of $\Upsilon(z)$ would be selected and a family of shape functions are derived from it by translation and dilation. The shape functions $f_m(z)$ are subsequently obtained as,

$$f_m(z) = \Upsilon\left(\frac{z - a_m}{b_m}\right) \quad (23)$$

The modulation function should be a smooth analytical non-linear function which results in the shape functions exhibiting the expected distribution that is experimentally observed (Korsunsky et al., 2008). To this end, an exponential form is selected for modulation function where $\Upsilon(z) = \exp(\gamma z)$. It should be noted that the shape function parameters are chosen on the basis of well-posedness of the solution considering relatively small condition number of the system and fast convergence rate of the solution. Thus for laser-forming residual field, the constant of $\gamma = -2$ and the sequence of $b_m = (1/2)^m$ is selected while it is assumed that a_m is constant and equal to the thickness of the plate. Therefore the explicit form of shape functions are given by,

$$f_m(z) = \exp(-2^{m+1}(z - h)) \quad (24)$$

The residual elastic strain distribution would now be reconstructed and exhibited in Fig. 4. The order of line-wise approximation used for reconstruction of residual elastic strain by variational inverse eigenstrain analysis is $M = 13$ (Korsunsky et al., 2008) while just $M = 6$ terms of non-linear shape functions are utilized in the smoothed inverse eigenstrain method. It is clearly deduced from Fig. 4 that the reconstructed R.E.S. by smoothed inverse eigenstrain approach has an excellent agreement with the measurements whereas some disagreement between the variational eigenstrain model and experimental data is observed (Korsunsky et al., 2008). Following the previously described regularization procedure, the regularized R.E.S. field by Tikhonov–Morozov and the gradient iterative method for laser-forming process are shown in Fig. 5. Again the gradient iterative regularization shows an excellent convergence to the Tikhonov–Morozov regularized results. Also the regularization parameter, iteration steps and regularization relative error for laser-forming R.E.S. are tabulated in Table 1 too.

As the last data set, the eigenstrain and residual stress distribution of shot-peened specimen is examined here. The aluminum alloy thick coupon has dimensions of $150 \times 50 \times 4$ mm and in tests is peened to full coverage (Levers and Prior, 1998). The eigenstrain and residual stress profile by the variational inverse eigenstrain analysis (Korsunsky, 2005) are shown in Figs. 6 and 7, respectively. Since data are available as the eigenstrain measurements, the truncated series form of the longitudinal eigenstrain as Eq. (9) is

Table 1
Regularization parameter, iteration steps and regularization relative error.

	Regularization parameter	Iteration steps	Relative error
Titanium bent bar	7.90542×10^{-5}	28	0.24994
Laser-formed steel plate	1.17995×10^{-4}	12	0.06165
Shot-peened thick coupon	4.95766×10^{-7}	19	0.04249

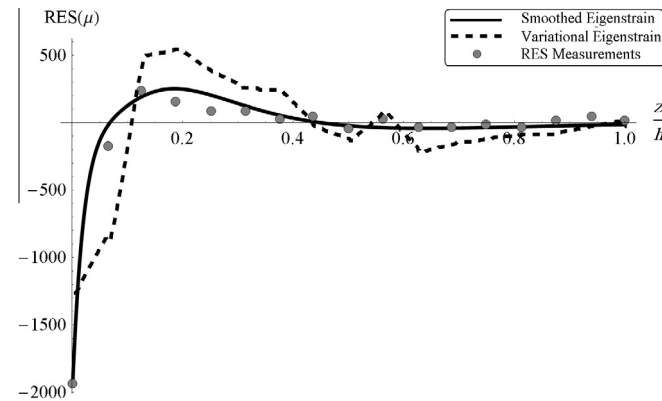


Fig. 4. R.E.S. measurements (Korsunsky et al., 2008) compared with the reconstructed R.E.S. by variational (Korsunsky et al., 2008) and smoothed inverse eigenstrain analysis.

utilized here. The shot peening residual stress field is also studied utilizing the stress function approach (Farrahi et al., 2009a) and the shape functions derived from exponential modulation function is shown to effectively satisfy the physical conditions of the shot peening process and exhibit the expected residual stress distribution. Therefore for the eigenstrain data shown in Fig. 6, eigenstrain base functions are determined according to $\psi_m^*(z) = \Upsilon\left(\frac{z-a_m}{b_m}\right)$ from an exponential modulation function of $\Upsilon(z) = \exp(\gamma z)$. Moreover based on the well-posedness of the solution considering relatively small condition number of the system and fast convergence rate of the solution, the constant of $\gamma = 6$ and the sequence of $b_m = (1/3)^m$ is selected while it is assumed that the sequence of a_m is constant and equal to the thickness of the specimen. Consequently the explicit form of eigenstrain base functions is given by,

$$\psi_m^*(z) = \exp\left(2 \times 3^{m+1}(z - h)\right) \quad (25)$$

Once the explicit form of the eigenstrain base functions is determined, the coefficients of the truncated series of the eigenstrain

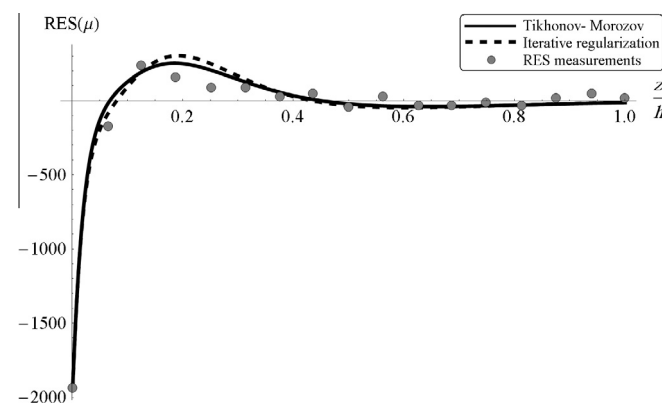


Fig. 5. R.E.S. measurements (Korsunsky et al., 2008) compared with the regularized reconstructed R.E.S. by Tikhonov–Morozov and gradient iterative regularization.

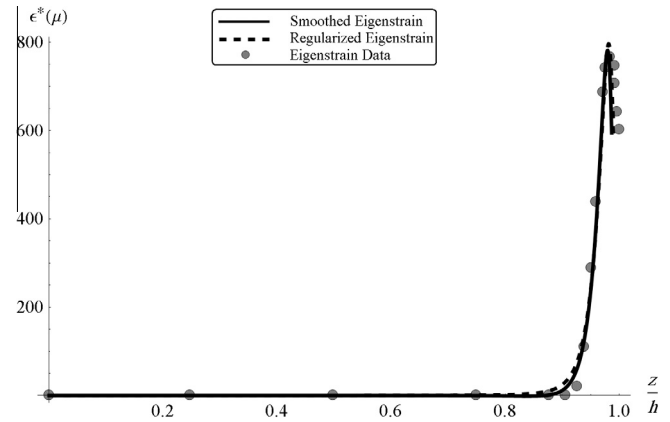


Fig. 6. Eigenstrain data (Korsunsky, 2005), reconstructed and Tikhonov–Morozov regularized eigenstrain field by smoothed inverse eigenstrain analysis.

field could be evaluated utilizing the least square analysis and the longitudinal eigenstrain profile given by Eq. (9) is reconstructed and exhibited in Fig. 6.

Subsequent to the reconstruction of eigenstrain field, the unknown coefficients of the linear total strain would be determined as Eq. (11) and consequently the R.E.S. and residual stress distribution would be evaluated as Eqs. (10) and (7), respectively. The reconstructed longitudinal residual stress profile is shown in Fig. 7. It is obviously inferred from Fig. 7 that the results of the smoothed inverse eigenstrain approach have an excellent agreement with the residual stress profile of the variational inverse eigenstrain analysis (Korsunsky, 2005) in the entire shot peening domain. The physical behavior of the longitudinal residual stress exhibits the expected distribution of residual stresses in shot peened plates that is in agreement with other shot peening results of thin specimens found in the literature (Miao et al., 2010). Also the reconstructed residual stress field has a fast convergence rate with just $M=9$ terms of smooth and appropriately localized base functions.

Once the eigenstrain field is reconstructed and the residual stress profile is determined, they may be regularized by Tikhonov–Morozov and gradient iterative regularization with replacing the R.E.S. shape functions with eigenstrain base functions in the regularization analysis. The regularized eigenstrain and residual stress field are shown in Figs. 6 and 8, respectively. The gradient iterative method once more shows an excellent convergence to the Tikhonov–Morozov regularization results. The regularization

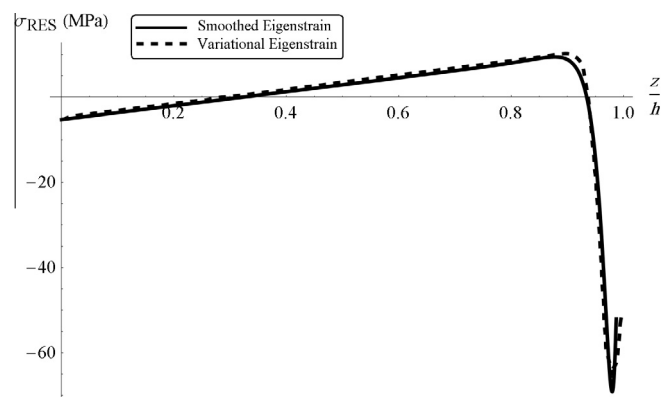


Fig. 7. Reconstructed residual stress field by smoothed inverse eigenstrain analysis compared with the variational inverse eigenstrain results (Korsunsky, 2005).

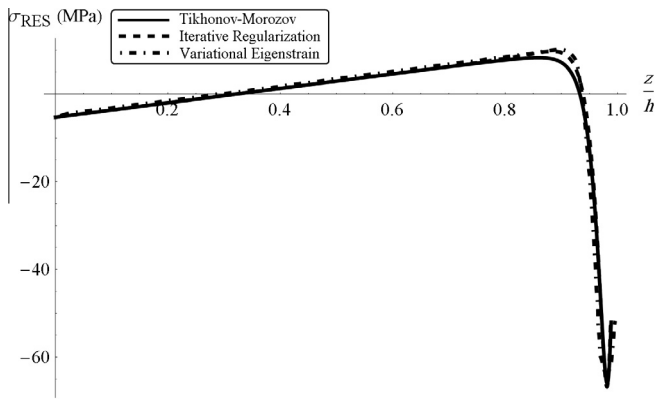


Fig. 8. Regularized reconstructed residual stress field by Tikhonov–Morozov and gradient iterative regularization compared with the variational inverse eigenstrain results (Korsunsky, 2005).

parameter, iteration steps and regularization relative error for shot peening eigenstrain field are also tabulated in Table 1.

It worth to note that, the main idea of regularization is to penalize large values in potential solutions, while still asking that the matching of the model output to data occurs to some degree (Engl et al., 1996). In all reconstructed residual fields, Tikhonov regularization method is shown to effectively reduce the influences of measurement noise without considerably distorting the reconstructed curve. Also it has been shown that the gradient iterative method examined here for regularization of the residual fields has an excellent convergence to the Tikhonov–Morozov regularization results. However the effect of regularization is more distinct on polynomial shape functions while the non-linear smooth shape functions seem to be more numerically stabilized. Moreover it should be noted that even if the gradient iterative methods do not utilize Tikhonov regularization parameter but Morozov discrepancy principle still has an important role for definition of stopping criterion of the iterative process.

4. Conclusion

A smoothed inverse eigenstrain method is developed in the present study for reconstruction of residual fields from limited residual strain and eigenstrain measurements. The well-rehearsed advantage of the proposed eigenstrain-based approach is that it not only minimizes the deviation of the residual measurements from its predicted values but also will result in an inverse solution satisfying the full range of continuum mechanics requirements (strain compatibility, stress equilibrium, traction free boundary conditions and vanishing the mean value on the entire domain). However, even within this class of solutions, different levels of smoothness can be obtained from minimization. The smoothed inverse eigenstrain approach allows suppressing oscillations or sharp gradients that are contrary to the physics of the problem. The analysis is successfully applied to three case studies where residual stresses have been introduced by inelastic beam bending, laser-forming and shot peening. It is shown that appropriate choice of shape functions based on the expected physical conditions of the process would results in stabilized numerical behavior. Also the smooth and non-singular base functions are achieved analytically without need to utilize numerical tools such as the finite element or boundary element methods. Furthermore a detailed discussion is made on the invertibility, uniqueness, well-posedness and convergence of the asymptotic residual field solution. The residual field solution is also regularized by Tikhonov–Morozov and gradient iterative method. The exact value of the regularization

parameter is then determined and it has shown that regularization effectively reduce the influences of measurement noise without considerably distorting the reconstructed profile. Furthermore it has been found that the gradient iterative method has an excellent convergence to the Tikhonov–Morozov regularization results.

Although in the present study, the analytical method is applied to one-dimensional residual data but it must be pointed out that the smoothed inverse eigenstrain approach is not limited to one-dimensional problems and can be generalized to higher-dimensional cases. The new analytical approach for determination of the residual fields therefore has the potential to provide significant improvement in the quality of residual data interpretation.

Acknowledgement

The author would like to acknowledge the valuable comments made by anonymous referee which were beneficial in the improvement of manuscript.

References

- Allaire, G., Kaber, S.M., 2008. *Numerical Linear Algebra*. Springer, New York.
- Bakushinsky, A.B., Kokurin, M.Y., Smirnova, A., 2011. *Iterative Methods for Ill-posed Problems: An Introduction*. Walter de Gruyter, Berlin.
- Cao, Y.P., Hu, N., Lu, J., Fukunaga, H., Yao, Z.H., 2002. An inverse approach for constructing the residual stress field induced by welding. *J. Strain Anal. Eng. Des.* 37 (4), 345–359. <http://dx.doi.org/10.1243/030932402760074562>.
- Cheney, E.W., 1982. *Introduction to Approximation Theory*. American Mathematical Society, Chelsea Publishing, New York.
- Coules, H.E., Smith, D.J., Venkata, K.A., Truman, C.E., 2014. A method for reconstruction of residual stress fields from measurements made in an incompatible region. *Int. J. Solids Struct.* 51 (10), 1980–1990. <http://dx.doi.org/10.1016/j.ijsolstr.2014.02.008>.
- Engl, H.W., Hanke, M., Neubauer, A., 1996. *Regularization of Inverse Problems*. Kluwer Academic Publishers Group, Dordrecht.
- Faghidian, S.A., 2013. New framework for Bayesian statistical analysis and interpolation of residual stress measurements. *Mech. Res. Commun.* 50, 17–21. <http://dx.doi.org/10.1016/j.mechrescom.2013.02.008>.
- Faghidian, S.A., Goudar, D., Farrahi, G.H., Smith, D.J., 2012a. Measurement, analysis and reconstruction of residual stresses. *J. Strain Anal. Eng. Des.* 47 (4), 254–264. <http://dx.doi.org/10.1177/0309324712441146>.
- Faghidian, S.A., Farrahi, G.H., Smith, D.J., 2012b. An analytical solution for inverse determination of residual stress field. *J. Solid Mech.* 4 (2), 114–127.
- Faghidian, S.A., Jozie, A., Sheykholo, M.J., Shamsi, A., 2014. A novel method for analysis of fatigue life measurements based on modified shepard method. *Int. J. Fatigue* 68, 144–149. <http://dx.doi.org/10.1016/j.ijfatigue.2014.05.009>.
- Farrahi, G.H., Faghidian, S.A., Smith, D.J., 2009a. An inverse approach to determination of residual stresses induced by shot peening in round bars. *Int. J. Mech. Sci.* 51 (9–10), 726–731. <http://dx.doi.org/10.1016/j.ijmecs.2009.08.004>.
- Farrahi, G.H., Faghidian, S.A., Smith, D.J., 2009b. Reconstruction of residual stresses in autofrettaged thick-walled tubes from limited measurements. *Int. J. Press. Vessels Pip.* 86 (11), 777–784. <http://dx.doi.org/10.1016/j.iijpvp.2009.03.010>.
- Farrahi, G.H., Faghidian, S.A., Smith, D.J., 2010. An inverse method for reconstruction of the residual stress field in welded plates. *J. Pressure Vessel Technol. Trans. ASME* 132 (6), 612051–612059. <http://dx.doi.org/10.1115/1.4001268>.
- Hill, M.R., 1996. *Determination of Residual Stress Based on the Estimation of Eigenstrain*. [Ph.D. Dissertation]. Stanford University.
- Hoger, A., 1986. On the determination of residual stress in an elastic body. *J. Elast.* 16 (3), 303–324. <http://dx.doi.org/10.1007/BF00040818>.
- Jun, T.-S., Korsunsky, A.M., 2010. Evaluation of residual stresses and strains using the eigenstrain reconstruction method. *Int. J. Solids Struct.* 47 (13), 1678–1686. <http://dx.doi.org/10.1016/j.ijsolstr.2010.03.002>.
- Kabanikhin, S.I., 2012. *Inverse and Ill-posed Problems: Theory and Applications*. Walter de Gruyter, Berlin.
- Korsunsky, A.M., 2005. On the modeling of residual stresses due to surface peening using eigenstrain distributions. *J. Strain Anal. Eng. Des.* 40 (8), 817–824. <http://dx.doi.org/10.1243/030932405X30984>.
- Korsunsky, A.M., 2006. Variational eigenstrain analysis of synchrotron diffraction measurements of residual elastic strain in a bent titanium alloy bar. *J. Mech. Mater. Struct.* 1 (2), 259–277. <http://dx.doi.org/10.2140/jomms.2006.1.259>.
- Korsunsky, A.M., 2009. Eigenstrain analysis of residual strains and stresses. *J. Strain Anal. Eng. Des.* 44 (1), 29–43. <http://dx.doi.org/10.1243/03093247JSA423>.
- Korsunsky, A.M., Regino, G.M., Nowell, D., 2007. Variational eigenstrain analysis of residual stresses in a welded plate. *Int. J. Solids Struct.* 44 (13), 4574–4591. <http://dx.doi.org/10.1016/j.ijsolstr.2006.11.037>.
- Korsunsky, A.M., Vorster, W.J.J., Zhang, S.Y., Topic, M., Venter, A.M., 2008. A beam bending eigenstrain analysis of residual elastic strains in multi-scan laser formed steel samples. *Proc. IMechE Part C J. Mech. Eng. Sci.* 222 (9), 1635–1645. <http://dx.doi.org/10.1243/09544062JMES750>.

- Levers, A., Prior, A., 1998. Finite element analysis of shot peening. *J. Mater. Process. Technol.* 80–81, 304–308. [http://dx.doi.org/10.1016/S0924-0136\(98\)00188-5](http://dx.doi.org/10.1016/S0924-0136(98)00188-5).
- Ma, H., Wang, Y., Qin, Q.-H., 2012. Determination of welding residual stresses by inverse approach with eigenstrain formulations of BIE. *Appl. Anal.* 91 (4), 807–821. <http://dx.doi.org/10.1080/00036811.2011.609986>.
- Miao, H.Y., Larose, S., Perron, C., Lévesque, M., 2010. An analytical approach to relate shot peening parameters to Almen intensity. *Surf. Coat. Technol.* 205 (7), 2055–2066. <http://dx.doi.org/10.1016/j.surfcoat.2010.08.105>.
- Morozov, V.A., 1984. *Methods for Solving Incorrectly Posed Problems*. Springer-Verlag, Berlin.
- Mura, T., 1987. *Micromechanics of Defects in Solids*. Kulwer Academic Publishers, Dordrecht, Netherlands.
- Nedin, R., Vatulyan, A., 2013. Inverse problem of non-homogeneous residual stress identification in thin plates. *Int. J. Solids Struct.* 50 (13), 2107–2114. <http://dx.doi.org/10.1016/j.ijsolstr.2013.03.008>.
- Qian, X.Q., Yao, Z.H., Cao, Y.P., Lu, J., 2004. An inverse approach for constructing residual stress using BEM. *Eng. Anal. Boundary Elem.* 28 (3), 205–211. [http://dx.doi.org/10.1016/S0955-7997\(03\)00051-1](http://dx.doi.org/10.1016/S0955-7997(03)00051-1).
- Samarskii, A.A., Vabishchevich, P.N., 2007. *Numerical Methods for Solving Inverse Problems of Mathematical Physics*. Walter de Gruyter, Berlin.
- Tikhonov, A.N., Arsenin, V.Y., 1977. *Solutions of Ill-posed Problems*. John Wiley & Sons, New York.
- Timoshenko, S.P., Goodier, J.N., 1970. *Theory of Elasticity*, third ed. McGraw-Hill, New York.
- Wimpory, R.C., Ohms, C., Hofmann, M., Schneider, R., Youtsos, A.G., 2009. Statistical analysis of residual stress determinations using neutron diffraction. *Int. J. Press. Vessels Pip.* 86 (1), 48–62. <http://dx.doi.org/10.1016/j.ijpvp.2008.11.003>.
- Withers, P.J., 2007. Residual stress and its role in failure. *Rep. Prog. Phys.* 70 (12), 2211–2264. <http://dx.doi.org/10.1088/0034-4885/70/12/R04>.
- Withers, P.J., Turski, M., Edwards, L., Bouchard, P.J., Buttle, D.J., 2008. Recent advances in residual stress measurement. *Int. J. Press. Vessels Pip.* 85 (3), 118–127. <http://dx.doi.org/10.1016/j.ijpvp.2007.10.007>.